Earth and Planetary Science Letters 449 (2016) 197–205

Contents lists available at ScienceDirect

Earth and Planetary Science Letters

www.elsevier.com/locate/epsl

Titanium stable isotope investigation of magmatic processes on the Earth and Moon

Marc-Alban Millet [a,b,*], Nicolas Dauphas [b], Nicolas D. Greber [b], Kevin W. Burton [a], Chris W. Dale [a], Baptiste Debret [a,1], Colin G. Macpherson [a], Geoffrey M. Nowell [a], Helen M. Williams [a,1]

[a] Durham University, Department of Earth Sciences, South Road, Durham DH1 3LE, United Kingdom
[b] Origins Laboratory, Department of the Geophysical Sciences and Enrico Fermi Institute, University of Chicago, 5734 S Ellis Avenue, Chicago, IL 60637, USA

ARTICLE INFO

Article history:
Received 22 July 2015
Received in revised form 28 April 2016
Accepted 24 May 2016
Available online xxxx
Editor: B. Buffett

Keywords:
stable isotopes
magma differentiation
bulk silicate Earth
lunar basalts

ABSTRACT

We present titanium stable isotope measurements of terrestrial magmatic samples and lunar mare basalts with the aims of constraining the composition of the lunar and terrestrial mantles and evaluating the potential of Ti stable isotopes for understanding magmatic processes. Relative to the OL–Ti isotope standard, the δ^{49}Ti values of terrestrial samples vary from −0.05 to +0.55‰, whereas those of lunar mare basalts vary from −0.01 to +0.03‰ (the precisions of the double spike Ti isotope measurements are ca. ±0.02‰ at 95% confidence). The Ti stable isotope compositions of differentiated terrestrial magmas define a well-defined positive correlation with SiO_2 content, which appears to result from the fractional crystallisation of Ti-bearing oxides with an inferred isotope fractionation factor of $\Delta^{49}Ti_{oxide-melt} = -0.23‰ \times 10^6/T^2$. Primitive terrestrial basalts show no resolvable Ti isotope variations and display similar values to mantle-derived samples (peridotite and serpentinites), indicating that partial melting does not fractionate Ti stable isotopes and that the Earth's mantle has a homogeneous δ^{49}Ti composition of +0.005 ± 0.005 (95% c.i., $n = 29$). Eclogites also display similar Ti stable isotope compositions, suggesting that Ti is immobile during dehydration of subducted oceanic lithosphere. Lunar basalts have variable δ^{49}Ti values; low-Ti mare basalts have δ^{49}Ti values similar to that of the bulk silicate Earth (BSE) while high-Ti lunar basalts display small enrichment in the heavy Ti isotopes. This is best interpreted in terms of source heterogeneity resulting from Ti stable isotope fractionation associated with ilmenite–melt equilibrium during the generation of the mantle source of high-Ti lunar mare basalts. The similarity in δ^{49}Ti between terrestrial samples and low-Ti lunar basalts provides strong evidence that the Earth and Moon have identical stable Ti isotope compositions.

1. Introduction

Much of the stable isotope variation seen on Earth is mass-dependent in nature, scaling as a function of the difference in mass of the isotopes involved. Departures from such mass-dependent isotope fractionation are, however, commonplace in meteorites (Clayton, 1993; Dauphas et al., 2002) and one of the most intriguing features of the Earth–Moon system is the similarity of their mass-independent isotope signatures (e.g.: O: Clayton et al., 1973; Cr: Lugmair and Shukolyukov, 1998; Ti: Zhang et al., 2012). This similarity is difficult to reconcile with simple giant impact models that predict that most of the Moon's mass should consist of impactor material, because in this case lunar rocks should have inherited the isotope composition of the impactor, which Pahlevan and Stevenson (2007) argued should have been different from that of the Earth. Different scenarios were proposed to explain this similarity ranging from isotope equilibration between Earth's mantle and the protolunar disk (Pahlevan and Stevenson, 2007), impact of a Mars-size body with a fast-spinning Earth (Cúk and Stewart, 2012), impact between two similar-sized protoplanets (Canup, 2012), "hit-and-run" impact (Reufer et al., 2012), or an Earth-like impactor (Dauphas et al., 2014a; Mastrobuono-Battisti et al., 2015). The wide range of physical processes invoked in each of these different models highlights the need to develop new tools to evaluate the consequences of each model on the chemical and isotopic evolution of the Moon with respect to the Earth.

Interestingly, and in contrast to many mass-independent isotope systems, the *mass dependent* stable isotope compositions of a

* Corresponding author at: School of Earth and Ocean Sciences, Cardiff University, Main building, Park Place, Cardiff CF10 3AT, United Kingdom.
E-mail address: milletm@cardiff.ac.uk (M.-A. Millet).
[1] Now at: Department of Earth Sciences, University of Cambridge, Downing Street, Cambridge CB2 3EQ, United Kingdom.

http://dx.doi.org/10.1016/j.epsl.2016.05.039
0012-821X/

number of elements in terrestrial and lunar samples display significant variations (e.g.: O and Fe: Liu et al., 2010; Poitrasson et al., 2004; Weyer et al., 2005; Mg: Sedaghatpour et al., 2013; Zn: Paniello et al., 2012; Li: Seitz et al., 2006; Cl: Sharp et al., 2010; Cr: Bonnand et al., 2016). The stable isotope compositions of these elements have the potential to shed new light on the evolution of the Earth–Moon system as their variations are diagnostic features of a variety of processes such as volatile element depletion, core formation, and magma ocean crystallisation. However, many of these non-traditional stable isotope systems are affected by multiple processes, which complicate their interpretation.

Titanium has the advantage of being both lithophile and extremely refractory. It is therefore unlikely to have been affected by formation of the lunar and terrestrial cores, or volatile element depletion during the giant impact. It thus has the potential to provide unambiguous constraints on lunar magma ocean crystallization. Despite its abundance in igneous rocks and the extensive use of TiO_2 concentrations in high-temperature geochemistry, Ti stable isotopes have received very limited attention to date (Millet and Dauphas, 2014; Zhang et al., 2014). Indeed, most of the studies so far focused on the detection of Ti isotopic anomalies to learn about nucleosynthetic processes, genetic relationships between planetary bodies, early solar system processes and/or cosmogenic effects (e.g.: Niederer et al., 1980; Niemeyer, 1988; Trinquier et al., 2009; Zhang et al., 2011, 2012). Titanium exists in several coordinations in magmatic systems: it is predominantly present in 5-fold coordination in all silicate melts but is also present in 4- and 6-fold coordinations in silicic and mafic melts respectively (Farges et al., 1996; Farges and Brown, 1997). In addition, 5-fold coordinated titanium transitions to 6-fold coordination during crystallisation of Ti-bearing oxides (Farges and Brown, 1997). As stable isotope theory (Schauble, 2004) predicts that stable isotope fractionation will be driven by major contrasts in elemental bonding environment, the coordination behaviour of Ti raises the possibility that Ti stable isotopes may serve as a tracer of magmatic processes. Furthermore, as Ti is refractory and comparably immobile in fluids, Ti stable isotopes are also likely to be comparatively resistant to overprinting. A potential complexity however, lies with the presence of Ti^{3+} in reduced magmas and planetary bodies such as the Moon. Oxygen fugacity estimates for the lunar mantle range from the iron–wüstite buffer to 2 log units below it (i.e. IW-2), with a most likely value of ∼IW-1 (Wadhwa, 2008). Experimental work has shown that in these conditions, the lunar mantle could contain up to 10% Ti^{3+} (Krawczynski et al., 2009). However, direct measurements of $Ti^{3+}/\Sigma Ti$ (Simon et al., 2014) in pyroxenes and olivines from lunar basalts have not detected any Ti^{3+}.

In this contribution, high precision Ti stable isotope measurements are presented for a range of terrestrial and lunar magmatic rocks with three aims. The objectives of this contribution are to (*i*) evaluate the effect of fractional crystallisation and magma differentiation on the Ti stable isotope composition of silicate melts; (*ii*) determine the Ti stable isotope composition of the terrestrial mantle and assess its homogeneity and (*iii*), use the Ti stable isotope composition of lunar basalts to investigate the magmatic evolution of the Moon.

2. Samples and methods

2.1. Samples

In addition to the dataset already presented in Millet and Dauphas (2014), we have analysed 36 terrestrial samples reflecting a global coverage from a diverse range of geodynamic contexts. We have also analysed 9 primitive lunar basalts covering the range of TiO_2 concentrations observed in lunar rocks.

Mid-Ocean Ridge Basalts (MORB). Seven MORB samples were analysed in order to constrain the composition of the upper mantle. The sample suite includes glasses from the mid-Atlantic ridge, the East-Pacific Rise (Batiza and Niu, 1992), the Pacific–Cocos–Nazca triple junction (Puchelt and Emmermann, 1983) as well as the South–West Indian Ridge (Escrig et al., 2004), including a single MORB sample displaying Sr, Pb and Os isotope compositions characteristic of the Dupal anomaly (MD57 9-1).

Island arc basalts. The island arc basalts studied here mainly comprise basalts sampled from oceanic arcs in order to limit the potential for crustal contamination and assimilation processes. In addition to the New Britain basalt data published by Millet and Dauphas (2014), 3 arc lavas from the Mariana arc were studied that were previously analysed for major and trace elements by Yi et al. (2000). A single basalt from the Izu–Bonin arc, rock standard JB-2, was also analysed.

Intraplate basalts. The intraplate basalts mainly comprise ocean island basalts (OIBs) from four different localities. Single samples from Hawaii (BHVO-2 rock standard) and Easter Island (sample 17678, Baker et al., 1974) were analysed as well as samples from the Cape Verde (São Nicolau island; Millet et al., 2008) and Azores archipelagos (São Miguel island: Turner et al., 1997; São Jorge island: Millet et al., 2009). In addition, a single continental flood basalt (the USGS rock standard BCR-2) was also analysed.

Eclogites. The three eclogites measured here were collected from the Zermatt-Saas Fee ophiolite, Switzerland. They consist of 2 basaltic eclogites and 1 gabbroic eclogite, based on their mineralogy (Dale et al., 2007). Estimates of peak metamorphic conditions for these samples range between 2 and 3 GPa and from 550 to 630 °C (Barnicoat and Fry, 1986; Reinecke, 1991). Major and trace element data (Dale et al., 2007) show that all the samples selected suffered loss of volatile and fluid-mobile elements during metamorphic dehydration.

Mantle samples. The mantle-derived samples are of two types. First, a single orogenic peridotite from the Beni Bousera massif was analyzed (GP13, Pearson et al., 2004). The other 3 mantle-derived samples are serpentinites from various Western Alps ophiolites. These samples originate from the lithospheric mantle section of a subducted slab and have been chosen because they record different metamorphic conditions during subduction. These have partly (BCh9, MM15) to fully (LZ14b) re-equilibrated in the antigorite (high temperature and pressure variety of serpentine) stability field during subduction (see Debret et al., 2014 for details).

Differentiated magmas. In order to assess the effect of magmatic differentiation, rock standards of varying SiO_2 content (AGV-1 andesite: 58.8 wt%, G-2 granite: 69.1 wt%, RGM-1 rhyolite: 73.4 wt%) and a basaltic andesite from São Miguel Island (54.5 wt% SiO_2, Azores archipelago) were analysed. Although not cogenetic, these samples span almost the full range of silica content observed in terrestrial rocks and show a continuous decrease in TiO_2 content with increasing SiO_2. To complement this sample set, 6 cogenetic samples from Agung volcano (Bali, Indonesia) related to each other by fractional crystallisation were analysed. The SiO_2 concentration of these samples ranges from 54 to ca. 63 wt% and TiO_2 shows a continuous decrease from 0.92 to 0.60 wt% over that range (Dempsey, 2012).

Lunar samples. Nine lunar samples were analysed. Specifically, we selected 5 high-Ti basalts (TiO_2 ranging from 12.2 to 13.4 wt%) and 3 low-Ti basalts (TiO_2 ranging from 1.9 to 3.3 wt%). A single green glass sample was also analysed (sample 15426, TiO_2 = 0.5 wt%).

2.2. Methods

Samples were processed and measured using the double-spike method of Millet and Dauphas (2014), which is briefly outlined

here. Between 10 to 50 mg of rock powder (for whole rock samples) or glass chips (for MORB glasses) were digested in a 1:1 mixture of concentrated HF and HNO_3 for 48 h. After careful evaporation, samples were then taken up in nitric acid and dried down 3 times before being taken up in 6 M HCl and checked for residual solids. If samples were fully digested, approximately 30 mg of H_3BO_3 was added to the solution in order to ensure that any potential fluorides (for which Ti has a strong affinity) having escaped visual inspection are re-dissolved and thus ensure that all the Ti contained in the sample is in solution. An aliquot containing 5 to 20 µg of Ti is then taken and mixed with a ^{47}Ti–^{49}Ti double spike in appropriate proportions (the Ti concentrations of the various rocks analysed were known from prior work). Purification of Ti was achieved following the procedure designed by Zhang et al. (2011) and using a two-step chemistry. Firstly, the samples were passed through a TODGA cartridge to remove almost all sample matrix. Samples were then further purified using AG1-X8 resin in order to separate Mo (thus limiting potential doubly charged interferences on Ti isotopes) and remaining Ca. It is notable that lunar samples and BHVO-2 rock standard were digested at the Origins Laboratory of the University of Chicago by flux fusion method using $LiBO_3$ as a fluxing agent. This was to ensure that potential refractory phases were fully digested. After fusion, samples are dissolved in 3 M HNO_3 before an aliquot containing 20 µg of Ti is taken and spiked in ideal proportions. Chemical purification of Ti was achieved using the procedure outlined above.

Isotope ratio measurements were carried out on Neptune Plus MC-ICP-MS installed in the Arthur Holmes laboratory at Durham University and at the Origins Laboratory of the University of Chicago. The samples were injected into the plasma torch using an Aridus II desolvating nebuliser and the isotope measurements were performed in medium resolution mode. Despite being double-spiked, all sample measurements were bracketed by measurements of double-spiked standards (OL–Ti) measured at the same concentration level in order to account for small unresolved polyatomic interferences on ^{47}Ti and ^{48}Ti produced in the mass spectrometer. Raw data is then processed offline using in-house double-spike deconvolution codes written in Mathematica®. All data is expressed as δ^{49}Ti, which is the deviation of the ^{49}Ti/^{47}Ti ratio of samples relative to that of the OL–Ti standard (Millet and Dauphas, 2014). This standard is available from the corresponding author upon request.

Finally, it should be noted that double-spike measurements rely on the assumption that the 4 isotopes used in the double-spike deconvolution routine are related to by mass-dependent stable isotope fractionation only. Double-spike method can provide inaccurate result if any of the isotopes involved is affected by mass-independent variation. To this day, no mass-independent variations have been found in terrestrial samples for Ti isotopes, but significant ^{50}Ti anomalies have been detected in lunar samples related to cosmic ray exposure. These anomalies could lead to potentially inaccurate results if not accounted for. For this reason, our double-spike deconvolution procedure uses ^{46}Ti, ^{47}Ti, ^{48}Ti, and ^{49}Ti that are only related to each other by mass-dependent fractionation in both terrestrial and lunar rocks.

3. Results

Data for all standards and samples analysed during the course of this study are given in Table 1. For samples measured once only, quoted errors are internal errors, whereas for samples measured multiple times, 95% confidence intervals were calculated using the Isoplot software (Ludwig, 2003). Repeated digestion and analysis of BCR-2, BHVO-2 (HF or flux fusion digestion) and JB-2 reference materials, previously analysed by Millet and Dauphas (2014) at the Origins Laboratory (University of Chicago), were conducted in order to certify data quality and the absence of inter-laboratory bias (Fig. 1). The average Ti isotope compositions of standards analysed at Durham University is in excellent agreement with that of the Origins Laboratory data and demonstrates that the 2σ reproducibility of our δ^{49}Ti measurements is ca. ±0.020‰. In addition, we have carried out replicate digestions and analysis of the RGM-1 rock standard (only in Durham) which all display values within analytical uncertainty (0.548 ± 0.014‰, 95% c.i., $n = 4$). Finally, for BHVO-2 rock standard, measurements of flux fusion digestions carried out in Chicago displays value within analytical uncertainty of HF–HNO_3 digestions performed in both Durham and Chicago (Greber et al., 2016; Fig. 1).

The δ^{49}Ti values of all terrestrial samples ranges from −0.046 to +0.548‰. Samples of differentiated magmas display a large range in Ti isotope compositions and an overall enrichment in isotopically heavy Ti isotopes (+0.054 to +0.548‰) relative to basalts and mantle-derived rocks (−0.046 to +0.049‰), which display more homogeneous compositions. In the MORB, OIB and IAB sample subsets, there appear to be no differences related to sampling localities.

Unlike primitive terrestrial samples, primitive lunar basalts display small but resolvable Ti stable isotope heterogeneity, which relates to their TiO_2 content. High-Ti basalts display overall heavier δ^{49}Ti values (+0.011‰ to +0.033‰) relative to those of low-Ti lunar basalts and the single green glass sample analysed (−0.008 to +0.011‰).

4. Discussion

Significant variations exist in the Ti stable isotope compositions of terrestrial and lunar magmatic samples (Table 1). Below, we discuss the probable causes of Ti stable isotope fractionation and evaluate the degree of homogeneity of the Earth's mantle in terms of Ti stable isotopes. We then focus on the variability observed in the Ti stable isotope composition of primitive lunar mare basalts and discuss the implications of these data for the magmatic evolution of the Moon.

4.1. Ti stable isotope fractionation during magma differentiation

A striking feature of our terrestrial sample dataset is the significant enrichment of differentiated magmatic rocks in isotopically heavy Ti isotopes relative to more primitive magmatic rocks. This enrichment is correlated with SiO_2 content, suggesting a relationship with fractional crystallisation processes (Fig. 2). Titanium is highly to moderately incompatible in most of the silicate minerals typically involved in magma differentiation (pyroxenes, olivine, plagioclase, micas, quartz) regardless of the composition of the melt. Mass balance considerations therefore suggest that it is unlikely that the crystallisation of silicate mineral phases could have modified the Ti isotopic composition of the remaining melt.

Titanium behaviour during fractional crystallisation is mainly controlled by the crystallisation of Fe–Ti oxides that can occur at all stages of magma differentiation. The coordination of Ti in silicate melts and oxide minerals was investigated by Farges et al. (1996) and Farges and Brown (1997). In silicate melts, Ti is predominantly present in 4, 5, and 6-fold coordinations, whereas Fe–Ti oxides exclusively accommodate 6-folded Ti (Farges et al., 1996). As stable isotope theory (Schauble, 2004) predicts that isotopically heavy species will be preferentially concentrated in low-coordination, high-force constant (stronger and stiffer) bonding environments, at equilibrium Fe–Ti oxides might thus display enrichments in isotopically light Ti relative to the co-existing melt. The progressive crystallisation of Fe–Ti oxides during magmatic differentiation could potentially, therefore, drive the residual melt to heavy isotope compositions.

Table 1
Ti stable isotope composition of samples measured during the course of this study. Data presented for samples replicated multiple times are weighted means and 95% c.i. calculated using Isoplot (Ludwig, 2003). For rock standards BHVO-2, BCR-2 and JB-2, averages represent the combination of data obtained by Millet and Dauphas (2014) and this study.

Type/locality	Sample	Lab	SiO_2	TiO_2	MgO	δ^{49}Ti	95% c.i.	*n*
MORB								
North Atlantic	A127D8-2	Dur	50.08	0.81	9.43	−0.003	0.020	1
North Atlantic	A127D11-1	Dur	51.1	1.17	8.55	0.006	0.020	1
EPR	R94-2	Dur	51.0	1.33	7.59	0.002	0.028	1
EPR	R82-1	Dur	49.3	1.06	9.17	0.002	0.014	1
Pacific	Sonne12 42a	Dur	49.93	1.5	8.23	0.005	0.021	1
Indian	MD57 9-1	Dur	51.87	0.98	8.88	−0.010	0.025	1
Indian	MD57 10-1	Dur	50.69	1.68	6.84	0.011	0.040	1
Island arc basalts								
Japan	JB-2	Dur/OL	53.2	1.19	4.66	−0.046	0.009	3
Marianas	ALV1846-9	Dur	49.67	0.57	6.95	0.008	0.017	1
Marianas	1883-5	Dur	52.26	0.77	5.46	0.049	0.013	1
Marianas	1885-6	Dur	54.6	0.79	5.8	0.036	0.018	1
Intraplate								
Columbia River	BCR-2	Dur/OL	54.1	2.26	3.59	−0.015	0.005	12
Easter	17678	Dur	47.79	2.97	7.79	−0.004	0.020	1
Hawaii	BHVO-2	Dur/OL	49.9	2.73	7.23	0.020	0.006	12
Cape Verde	SN01	Dur	41.01	2.88	15.09	0.005	0.022	1
Cape Verde	SN10	Dur	39.88	2.90	12.50	0.008	0.022	1
Azores	S1	Dur	45.31	4.09	7.76	0.026	0.027	1
Azores	S3	Dur	46.43	3.59	8.34	0.037	0.018	1
Azores	SJ52	Dur	44.35	3.78	8.20	0.017	0.018	1
Eclogites								
Zermatt-Saas	SO241ii	Dur	47.14	2.75	5.20	−0.015	0.025	1
Zermatt-Saas	SO241v 2	Dur	49.04	2.72	5.51	0.004	0.031	1
Zermatt-Saas	SO284viix	Dur	49.9	0.7	8.8	−0.025	0.025	1
Mantle-derived								
Alpine serpentinite	Bch9	Dur	40.21	0.09	36.04	0.012	0.031	1
Alpine serpentinite	MM15	Dur	39.53	0.06	36.34	−0.003	0.028	1
Alpine serpentinite	LZ14b	Dur	39.03	0.07	38.13	0.030	0.023	1
Beni Bousera peridotite	GP13	Dur	44.91	0.14	39.79	0.007	0.022	1
Differentiated magmas								
Basaltic andesite	S19	Dur	54.49	2.11	6.38	0.103	0.022	2
Andesite	AGV1	Dur	58.84	1.05	1.53	0.084	0.029	2
Granite	G2	Dur	69.14	0.48	0.75	0.459	0.027	2
Rhyolite	RGM1	Dur	73.4	0.27	0.275	0.548	0.014	4
Agung	AGU03	Dur	58.01	0.76	2.92	0.120	0.027	1
Agung	AGU16	Dur	59.93	0.7	2.3	0.179	0.029	1
Agung	AGU20	Dur	62.69	0.6	1.77	0.248	0.032	1
Agung	AGU21	Dur	54.08	0.92	4.13	0.054	0.026	1
Agung	AGU23	Dur	56.42	0.76	2.95	0.108	0.029	1
Agung	AGU25	Dur	65.16	0.55	1.46	0.259	0.019	1
Moon								
High-Ti	70017	OL	–	13.3	–	0.015	0.011	5
High-Ti	70215	OL	–	13.0	–	0.033	0.015	5
High-Ti	71055	OL	–	13.4	–	0.011	0.017	5
High-Ti	72155	OL	–	12.2	–	0.023	0.009	5
High-Ti	75075	OL	–	13.4	–	0.018	0.014	5
Low-Ti	15597	OL	–	1.85	–	−0.008	0.010	5
Low-Ti	12009	OL	–	3.30	–	−0.008	0.013	5
Low-Ti	15016	OL	–	2.30	–	−0.008	0.019	4
Green glass	15426	OL	–	0.50	–	0.011	0.017	4

In order to test this hypothesis, we have modelled the evolution of a primitive basaltic melt to a silicic composition by fractional crystallisation using Rhyolite MELTS software (Gualda et al., 2012). The composition of the starting material is set to be similar to that of arc basalts (see Fig. 2 caption), crystallisation occurs at 1 kbar and the relative oxygen fugacity is assumed to be constant at the NNO buffer. At each calculation step, the compositions and respective mass of melt and minerals in equilibrium are calculated. Steps are defined by a 5 °C incremental temperature decrease from the liquidus temperature (here 1118 °C). The calculation stops when the temperature reaches 900 °C, at which point ca. 70% of the liquid has crystallised and the SiO_2 content of the remaining liquid has reached 66 wt%. The Ti isotope evolution of the melt is calculated, at each step, using a Rayleigh distillation law and a bulk Ti stable isotope fractionation factor between the residual melt and the minerals removed. As silicate minerals have a negligible effect on the budget of Ti in differentiating magmas, their contribution to the Ti isotope evolution of the residual melt must also be negligible. Consequently, the bulk melt–residue Ti stable isotope fractionation factor is equal to that between Fe–Ti oxides and melt ($\Delta^{49}Ti_{oxide-melt}$) weighted according to the relative proportion of Ti sequestered by oxides at each temperature step. Assuming that the fractionation is equilibrium in nature, the model reproduces the observed trend in δ^{49}Ti vs. SiO_2 well for an empirical value of $\Delta^{49}Ti_{oxide-melt} = -0.23‰ \times 10^6/T^2$ (with T in K) indicating that fractional crystallisation of Fe–Ti oxides is a viable

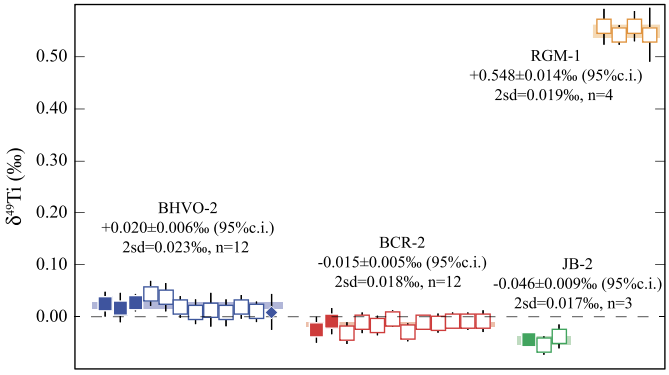

Fig. 1. δ^{49}Ti values of BHVO-2, BCR-2 and JB-2 basaltic rock standards measured during the course of this study. Filled symbols represent data generated at the Origins Laboratory and published in Millet and Dauphas (2014), while open symbols represent data obtained at Durham University. For BHVO-2, measurement made after flux fusion digestion carried out in Chicago is represented as a filled diamond. Data for all rock standards are in excellent agreement between the two laboratories.

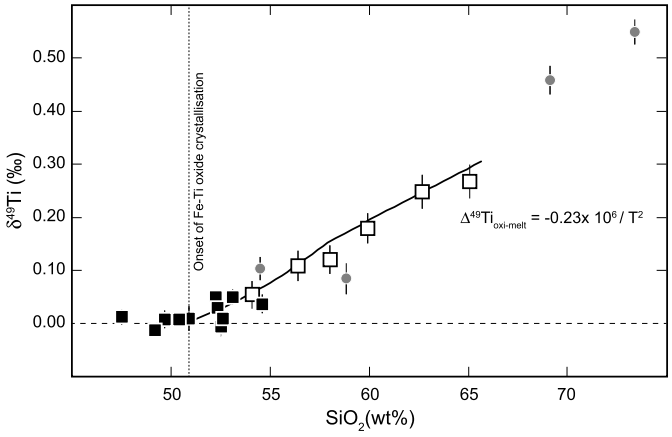

Fig. 2. Evolution of δ^{49}Ti values with SiO_2 concentration (wt%) of magmatic rocks. Arc basalts are in black squares whereas samples form the Agung volcano differentiation suite are in white squares. Other differentiated magmatic rocks are in grey circles. The budget of titanium during magma differentiation is controlled by the ongoing fractional crystallisation of isotopically light Ti oxides. Black curve represents the fractional crystallisation model generated using rhyolite–melts (see full text for details) and designed to fit the Agung Volcano cogenetic sample set. Starting melt composition (in wt%) is set at SiO_2: 50; TiO_2: 1; Al_2O_3: 18.5; FeO_{tot}: 11; MnO: 0.2; MgO: 5.5; CaO: 9; Na_2O: 2.5; K_2O: 0.7; P_2O_5: 0.2; H_2O: 1.8. Best fit for the data is obtained using a Ti stable isotope fractionation factor between oxides and melts of $\Delta^{49}Ti_{oxide-melt} = -0.23 \times 10^6/T^2$.

mechanism to explain the progressive enrichments of magmas in isotopically heavy Ti with increasing silica content. The predicted fractionation between oxide and melt at 900 °C is −0.167‰ for δ^{49}Ti. For comparison, Nuclear Resonant Inelastic X-ray Scattering (NRIXS) force constant measurements predict an equilibrium iron isotope fractionation between ilmenite (Krawczynski et al., 2013) and Fe^{2+}-bearing basaltic glasses (Dauphas et al., 2014b) at the same temperature of −0.09‰ for δ^{56}Fe (i.e., −0.05‰/amu). The equilibrium Ti isotope fractionation factor between oxide and melt that is needed to account for Ti isotope variations in silicic rocks is thus very reasonable. It should be noted that our preferred model does not account for any potential dependence of the Ti stable isotope fractionation factor on melt or Fe–Ti oxide chemical composition. Experimental work as well as measurements of oxide minerals in well-characterised sample suites will be needed to ascertain the oxide–melt isotopic fractionation factor inferred from measurements of differentiated terrestrial rocks.

The origin of the heavy Fe isotopic composition of silicic rocks with >70 wt% has been the subject of some debate. The explanations proposed thus far include iron mobilization by exsolved fluids (Poitrasson and Freydier, 2005; Heimann et al., 2008; Telus et al., 2012), Soret migration (Lundstrom, 2009), and fractional crystallization (Telus et al., 2012; Sossi et al., 2012; Dauphas et al., 2014b). For most silicic rocks, fluid exsolution is unlikely to be the culprit because more fluid mobile Zn does not display correlated fractionation and iron isotope enrichments also affect anhydrous A-type granites (Telus et al., 2012; Sossi et al., 2012). The finding of significant isotope variations for a fluid-immobile element like Ti in silicic magmatic rocks supports the view that fractional crystallization can drive stable isotope fractionations in transition metals. Iron and titanium stable isotope variations in magmatic rocks probably bear considerable insights into the processes governing magmatic evolution but equilibrium fractionation factors between minerals and melts need to be better know to reap the fruits of those studies.

4.2. The Ti stable isotope composition of terrestrial basalts and the Bulk Silicate Earth

Basaltic magmas display less variation in δ^{49}Ti relative to differentiated magmas (ca. 0.1‰ compared to ca. 0.6‰; Fig. 3). The variation observed is statistically significant (relative to analytical precision) and may be related to heterogeneity of the terrestrial mantle or other processes. However, the full range of basalt δ^{49}Ti variability is also observed in subduction zone basalts at the high end of the SiO_2 range (52–54 wt%). Two of the basaltic lavas from the Marianas and one New Britain sample display the heaviest Ti stable isotope compositions of all the basalts analysed, whereas the JB-2 rock standard (Izu–Bonin arc) displays the lightest composition of the entire sample set. Other basalt samples from the New Britain and Mariana arcs, which have lower silica contents, all display δ^{49}Ti values within analytical uncertainties, indicating that these three samples may have already been affected by the early onset of Fe–Ti oxide fractionation and are thus not representative of the Ti stable isotope composition of the sub arc mantle anymore. Fractional crystallisation cannot however explain the composition of the JB-2 rock standard, as no mineral phase typically involved during basaltic melt differentiation (e.g. olivine, pyroxenes, plagioclase, spinel, garnet) has been identified to preferentially incorporate the heavy isotopes of titanium relative to melt at equilibrium. As an arc basalt, JB-2 is expected to display anomalously low abundances of fluid immobile elements such as Ti and Nb relative to elements of similar incompatibility (Sm and Tb for Ti, Th and La for Nb; $Ti/Ti^* = Ti_N/\sqrt{Sm_N \times Tb_N}$ and $Nb/Nb^* = Nb_N/\sqrt{Th_N \times La_N}$, concentrations are normalised to the primitive mantle composition of McDonough and Sun, 1995) in normalised trace element patterns. For example, compiled data for the Izu–Bonin arc eruptives (obtained from Georoc database) show that at similar SiO_2 contents to JB-2 (53.2 wt%), Izu–Bonin magmas typically have Ti/Ti^* of 0.7 to 0.85 and Nb/Nb^* of 0.16 to 0.35. While JB-2 displays the strong negative Nb anomaly ($Nb/Nb^* = 0.21$) expected for island arc lavas, it does not display a negative Ti anomaly ($Ti/Ti^* = 1.02$). This feature can be explained by oxide accumulation in this sample. In contrast to Ti, Nb does not partition into Fe–Ti oxides (Nielsen and Beard, 2000) and therefore the accumulation of Fe–Ti oxides would lead to decoupling of Ti and Nb concentrations as well as enrichment in light isotopes of titanium.

Once samples that are affected by Fe–Ti oxide crystallisation or accumulation are removed (i.e. most silicic lavas from the Mariana arc, the most silicic New Britain sample and JB-2 rock standard), the average δ^{49}Ti values for island arc ($+0.007 \pm 0.010$‰, 95% c.i., $n = 8$), intraplate ($+0.009 \pm 0.019$‰, 95% c.i., $n = 7$) and mid-ocean ridge basalts ($+0.001 \pm 0.008$‰, 95% c.i., $n = 7$) are all within statistical error of each other and within our analytical uncertainty (see Fig. 1). Titanium behaves as a moderately incompatible ele-

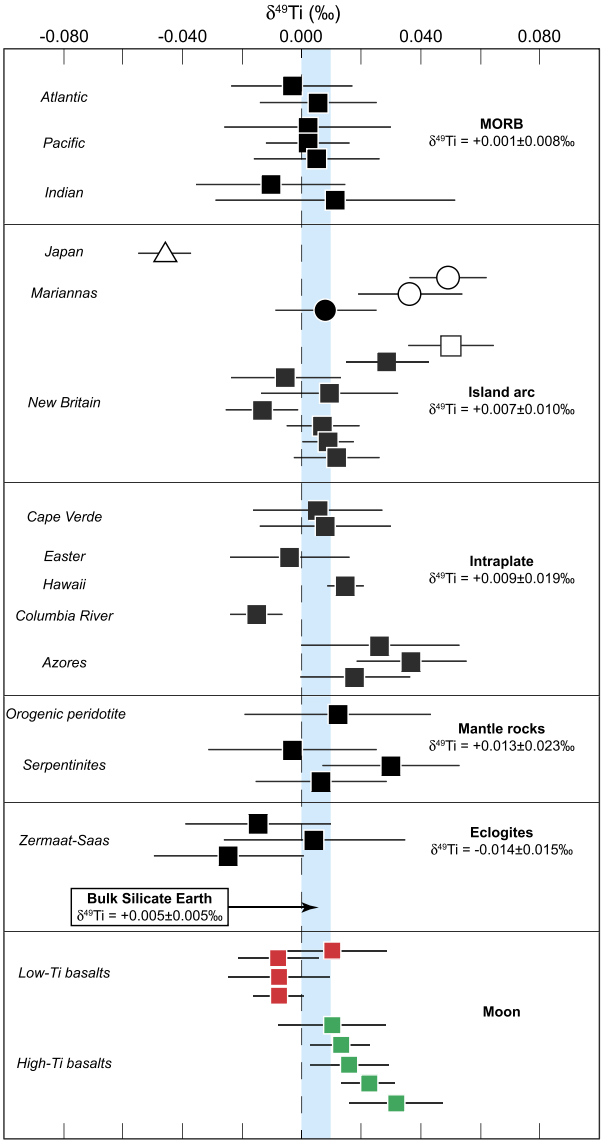

Fig. 3. Ti stable isotope compositions (δ^{49}Ti relative to OL-Ti) of terrestrial basalts, mantle-derived samples and eclogites as well as lunar mare basalts. Weighted means and 95% c.i. are calculated using Isoplot (Ludwig, 2003). Data for New Britain samples are from Millet and Dauphas (2014). Samples represented with open symbols show signs of fractionation or accumulation of Ti oxides based on TiO_2 concentrations and are removed from the calculation of the ^{49}Ti value of the BSE. Once these samples are removed, the δ^{49}Ti terrestrial igneous rocks show no resolvable variation between sampling location or geological context or petrographic type, indicating that the BSE has homogeneous Ti stable isotope composition of $+0.005 \pm 0.005$‰ relative to OL–Ti (95% c.i.). Low-Ti lunar basalts (red) show δ^{49}Ti values within error of the BSE whereas High-Ti mare basalts (green) show values ranging form BSE to enriched in heavy isotopes. (For interpretation of the references to colour in this figure legend, the reader is referred to the web version of this article.)

ment during melting of either spinel or garnet-bearing peridotite (Prytulak and Elliott, 2007) and is efficiently extracted from the mantle during basalt genesis. Mass-balance considerations thus dictate that basalts should record the Ti isotopic composition of their mantle source, unless melting occurs under Ti-oxide saturation. Our data on primitive basalts therefore indicates that the Earth's upper mantle has a homogeneous Ti stable isotope composition, within the precision of our measurements. In addition, the fact that the average value of our mantle samples (Beni Bousera Orogenic peridotite and Western Alps serpentinites) is indistinguishable from the average of all the primitive basalts analysed ($\delta^{49}Ti_{basalts} = +0.006 \pm 0.006$‰, 95% c.i., $n = 22$ vs. $\delta^{49}Ti_{mantle} = +0.013 \pm 0.023$‰, 95% c.i., $n = 4$) suggests that the partial melting of typical mantle lithologies (olivine + clinopyroxene + orthopyroxene + spinel and/or garnet) does not fractionate Ti stable isotopes.

In the bulk silicate Earth, Ti is mainly hosted in the mantle with only a minor proportion stored the continental crust (McDonough, 1991). It is therefore possible to calculate the Ti stable isotope composition of the Bulk Silicate Earth as the variance-weighted mean of primitive basalts, eclogites and mantle-derived samples analysed in this study, which yields a δ^{49}Ti value for the BSE (bulk silicate Earth) of $+0.005 \pm 0.005$‰ (95% c.i., $n = 29$). It is worth noting that measurement of a fully processed OL–Ti standard (digestion + chemical purification) shows that the analytical method used generates accurate results at the $\sim \pm 0.012$‰ precision level (Millet and Dauphas, 2014), so it is unknown if the δ^{49}Ti of the BSE value is accurate at the ± 0.005‰ level.

It is notable that primitive island arc basalts and MORBs display the same Ti stable isotope compositions. The mobility of Ti and other high-field-strength elements in subduction zone systems is a highly debated subject that mainly revolves around the stability of Ti-bearing phases during metamorphism of the down-going slab and the nature and composition of fluids in associated dehydration (e.g. Kessel et al., 2005). Experimental constraints have shown that rutile has low solubility in pure-H_2O fluids (Audetat and Keppler, 2005) and that the rutile–aqueous fluid partition coefficients for Ti, Nb and Ta are very high (Brenan et al., 1994). However, the presence of rutile in fluid-related mineral veins of deep-subducted rocks (Gao et al., 2007) indicates potential mobility of Ti and other HFSE in subduction zone environments. This is corroborated by recent experimental work on fluorine and chlorine-rich fluids (Rapp et al., 2010) and albite-saturated fluids (Antignano and Manning, 2008) in which Ti and other HFSE appear to be orders of magnitude more soluble than in pure-H_2O fluids. It is unclear in what speciation Ti is present in such fluids and it is thus hard to predict the direction and magnitude of stable isotope fractionation between rutile and co-existing fluids. Nevertheless, the bonding environment of Ti in halogen or Na-bearing fluids will be different to that of rutile and it is expected that this process will generate stable isotope fractionation. The identical average Ti stable isotope composition of MORBs and island-arc basalts therefore indicates that, even if Ti is mobilised during dehydration in subduction zones, this process does not affect the budget of Ti across the whole mantle wedge. Moreover, the fact that the eclogites and subduction-related serpentinites measured during this study display the same Ti isotope composition as MORBs ($\delta^{49}Ti_{eclogites} = -0.014 \pm 0.015$‰, 95% c.i., $n = 3$ and $\delta^{49}Ti_{serpentinites} = +0.016 \pm 0.043$‰, 95% c.i., $n = 3$) despite having been extensively dehydrated argues against significant mobility of Ti in subduction zones and hints that recycling of oceanic lithosphere may not generate detectable Ti stable isotope variation within Earth's mantle.

4.3. Titanium stable isotope heterogeneity of the lunar mantle as a consequence of the LMO crystallisation

Although limited in range, it appears that lunar mare basalts display slightly variable Ti stable isotope composition (Fig. 3). This variability is due to the heavier isotope composition of the high-Ti lunar basalts (Fig. 3). Titanium is an extremely refractory element that only partitions into gaseous phases at exceedingly high temperatures (Zhang et al., 2014). It is therefore unlikely that the difference between the two classes of lunar basalts is a consequence of evaporation during eruptive processes, neither can it be due to silicate–metal segregation as core formation in both the Earth and Moon took place under conditions that were too oxidising for titanium to partition into the core (Wade and Wood, 2001). The

titanium stable isotope variability observed in lunar basalts must therefore be related to processes that took place during the magmatic evolution of the Moon.

The source of High-Ti basalts are thought to be genetically linked to ilmenite-bearing cumulates formed between 95% and 99.5% solidification of the LMO (e.g. Snyder et al., 1992) as opposed to the sources of Low-Ti basalts that are formed earlier (<85% solidification) in the solidification sequence of the LMO before the onset of ilmenite crystallization (e.g. Hallis et al., 2014). Other minerals present in lunar mantle sources are olivine and pyroxenes, in which Ti is highly to moderately incompatible. Low-Ti lunar basalts display δ^{49}Ti values that are indistinguishable from that of the Earth's mantle. Results on terrestrial basalts undersaturated in Fe–Ti oxides (SiO_2 <52 wt% in Fig. 2) as well as mantle samples shows that olivine and pyroxenes do not fractionate Ti stable isotopes during fractional crystallisation or partial melting (Farges et al., 1996). Thus, low-Ti lunar basalts provide the best estimate of the Ti stable isotope composition of the lunar mantle, which is $\delta^{49}\text{Ti} = -0.003 \pm 0.014‰$ ($n = 4$) which is within statistical error to that of the Earth's mantle. Importantly, preliminary data for ordinary, enstatite and carbonaceous chondrites (Williams et al., 2014; Greber et al., 2016) also show uniform δ^{49}Ti within error of the Earth's mantle ($\delta^{49}\text{Ti} = +0.004 \pm 0.010‰$; Greber et al., 2016). Taken overall, the data for terrestrial, lunar and meteoritic samples available to date is consistent with recent models arguing for an Earth-like composition of the Moon-forming impactor (Dauphas et al., 2014a; Mastrobuono-Battisti et al., 2015).

As Fe–Ti oxide, ilmenite hosts six-fold Ti in its structure and is thus expected to preferentially incorporate light isotopes relative to melts at equilibrium as can be inferred from measurements of terrestrial silicic rocks. This behaviour provides an opportunity to test the models proposed for the generation of high-Ti lunar basalts. If all models agree on the involvement of an ilmenite-pyroxene cumulate layer in the late stages of LMO solidification, the details of the signatures of those cumulates were incorporated in high-Ti mare basalts is still a matter of debate. One view argues that high-Ti lunar basalts are derived from low-Ti lunar basalts through assimilation of ilmenite and pyroxene during magma ascent to the surface (Wagner and Grove, 1997). However, experimental work regarding the kinetics of assimilation of pyroxene and ilmenite suggests that ilmenite does not dissolve fast enough relative to pyroxene to generate compositions similar to high-Ti basalts (Van Orman and Grove, 2000) and would instead generate melt composition too rich in calcium. The other view involves the fertilisation of deep-seated ilmenite-free cumulates (i.e. formed earlier during the solidification of the LMO) by sinking ilmenite-bearing cumulates (Hess and Parmentier, 1995; Hallis et al., 2014). Concerns regarding the buoyancy of magmas generated by such sources as well as the elevated viscosity of the ilmenite-rich layer have lead to the formulation of a third model. Instead of solid-state mixing, this last model argues for fertilisation of the ilmenite-free cumulates by negatively buoyant partial melts of the ilmenite-rich layer formed as a result of the late heavy bombardment (Van Orman and Grove, 2000; Elkins-Tanton et al., 2002, 2004).

In order to test the solid-state mixing and the partial-melt fertilisation models, we modelled the evolution of the LMO during the crystallisation of the ilmenite-rich layer and examined its impact on the Ti stable isotope composition of high-Ti lunar melts. We assume a Ti concentration of 3 wt% at 95% PCS and mineral proportions similar to Snyder et al. (1992). At all steps of calculations, we calculate the Ti concentrations as well as the δ^{49}Ti of the residual melt, instantaneous cumulates as well as the bulk cumulate. We use the oxide–melt Ti isotope fractionation factor calculated in section 4.1 as a proxy for the ilmenite-melt fractionation factor. A simple Rayleigh distillation model ($T = 1125\,°C$;

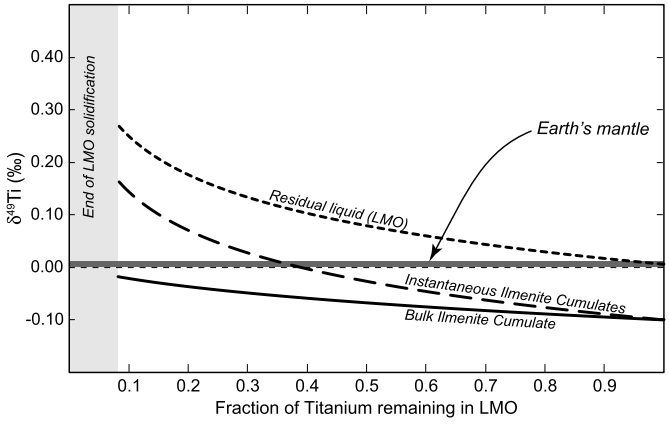

Fig. 4. Rayleigh distillation model showing the effect of ilmenite crystallisation during the late stages of solidification of the Lunar Magma Ocean. The ilmenite–melt Ti stable isotope fractionation factor is assumed to be equal to the oxide–melt fractionation factor calculated form the Agung volcano differentiation suite. Temperature is set at 1125 °C and mineral proportions are taken from Snyder et al. (1992). Partition coefficients for Ti for the mineral phases are set as follows: Ilmenite: 20; Clinopyroxene: 0.15; Pigeonite: 0.15 and Plagioclase: 0.

Van Orman and Grove, 2000) allows us to estimate the Ti stable isotope composition of the ilmenite-rich layer and evolving magma (Fig. 4). Calculations are stopped at 99.5% solidification, at which point 0.25 wt% Ti remains in the liquid. Overall, modelled ilmenite-bearing cumulates vary from −0.107‰ to +0.175‰. The remaining liquid at the end of ilmenite crystallisation is strongly enriched in heavy isotopes ($\delta^{49}\text{Ti} = +0.288‰$).

For the solid–state mixing model, we followed calculations by Hallis et al. (2014) who argued that high-Ti lunar basalt sources formed by mixing ilmenite-free cumulate made at 80% PCS with cumulates formed at 95% PCS (earliest ilmenite cumulates) in 80:20 proportions, this mixture is then topped up with 1% of trapped instantaneous residual liquid (TIRL at 95% PCS). Assuming Ti concentrations of 0.5 wt% and 6 wt% for the respective cumulates and 2.6 wt% for the liquid (based on our LMO solidification model), it is possible to estimate a δ^{49}Ti of the high-Ti lunar basalts mantle sources of −0.068‰. Interestingly, solid-state mixing models for the generation of high-Ti lunar basalts imply that ilmenite is exhausted during the generation of high-Ti melts (Ringwood and Kesson, 1976; Elkins-Tanton et al., 2002). Mass balance suggests that melts generated this way should display a δ^{49}Ti identical to that of their source and therefore lighter than low-Ti lunar basalts, contrary to our measurements. However, if ilmenite was not exhausted during partial melting, high-Ti lunar basalts should display heavier isotope composition than this modelled source. Uncertainty on the kinetics of ilmenite dissolution during lunar mantle melting to make high-Ti mare basalts makes further modelling difficult. Nevertheless, if ilmenite was a residual phase during generation of high-Ti magma, one may expect a negative relationship between Ti content and δ^{49}Ti of high-Ti lunar basalts. Such relationship does not appear in our data but this may be due to the relatively homogeneous TiO_2 content of the samples measured here (12.2 to 13.4 wt%) compared to the full range shown by high-Ti lunar basalts.

An alternative to direct mixing of isotopically light ilmenite-bearing cumulates into the sources of low-Ti lunar basalts is the fertilisation of these sources by negatively buoyant partial melts of these cumulates. This partial melting may have occurred as a result of the late heavy bombardment, directly through shock melting but also by adiabatic melting cause by the incurred mantle convection. Regardless of the process involved, our results predict that these partial melts should be enriched in heavy isotopes of Ti relative to the residue. Quantitative constraints on the composition of these

melts is currently lacking but as such, this model may provide a straightforward way to generate lunar mantle source with both elevated Ti content and heavy Ti stable isotope composition

5. Conclusion

This study presents the first investigation of the stable Ti isotope compositions of terrestrial and lunar igneous rocks. The main conclusions of this study are:

- The Ti stable isotope composition of terrestrial magmas shows a large variability that appears to be positively correlated with SiO_2 content. This is most likely the result of crystallisation of isotopically light Ti-oxides during magmatic differentiation with $\Delta^{49}Ti_{oxide-melt} = -0.23‰ \times 10^6/T^2$; $-0.106‰$ at 1200 °C). This observed fractionation is in agreement with the relative coordination of Ti between oxide minerals and silicate melts but further experimental data is needed to ascertain this value and assess whether it is equilibrium or kinetic in nature.
- The average δ^{49}Ti values of primitive mid-ocean ridge, island-arc and intraplate basalts are identical within our analytical uncertainties (ca. $\pm 0.020‰$). In addition, a preliminary set of mantle-derived samples also show δ^{49}Ti values within error of primitive terrestrial basalts. This demonstrates that little Ti stable isotope fractionation occurs during partial melting, and suggests that Earth's mantle (and the by extension the bulk Earth because no Ti is in the core) has a homogeneous Ti stable isotope composition of $\delta^{49}Ti_{BSE} = +0.005 \pm 0.005‰$ (95% c.i., $n = 29$).
- The lack of any significant fractionation of Ti stable isotopes between MORBs, and island-arc basalts, as well as eclogites and serpentinites form subduction zones argues against a significant mobility of Ti in fluorine or chlorine bearing fluids across the mantle wedge during dehydration of downgoing slabs.
- Finally, primitive lunar basalts possess Ti stable isotope compositions ranging from terrestrial values to slightly enriched in heavy isotopes (δ^{49}Ti up to $+0.033 \pm 0.015‰$). Low-Ti lunar basalts all display δ^{49}Ti values within error of the terrestrial mantle value whereas high-Ti lunar basalts display small but distinct enrichment in isotopically heavy Ti. The heavy δ^{49}Ti values recorded in high-Ti mare basalts indicate that their mantle source regions may have been fertilised either by ilmenite cumulates formed in the latest stages of the LMO or by negatively buoyant partial melts of ilmenite-bearing cumulates during the Late Heavy Bombardment.

Acknowledgements

MAM acknowledges financial support from Durham University and a Marie Curie COFUND International Junior Fellowship held at Durham University. ND was supported by grants from NSF (EAR 1144429, 1444951, 1502591) and NASA (NNX12AH60G, NNX14AK09G, NNX15AJ25G). NDG was supported by the Swiss National Science Foundation (grant P2BEP2-158983). HMW acknowledges support from NERC Advanced Fellowship NE/F014295/2 and the ERC (Consolidator Grant "HabitablePlanet" 306655). Collection and initial analysis of Agung samples was possible through funding from the SE Asia Research Group at Royal Holloway University of London.

References

Antignano, A., Manning, C.E., 2008. Rutile solubility in H_2O, H_2O–SiO_2, and H_2O–$NaAlSi_3O_8$ fluids at 0.7–2.0 GPa and 700–1000 °C: implications for mobility of nominally insoluble elements. Chem. Geol. 255, 283–293.

Audetat, A., Keppler, H., 2005. Solubility of rutile in subduction zone fluids, as determined by experiments in the hydrothermal diamond anvil cell. Earth Planet. Sci. Lett. 232, 393–402.

Baker, P.E., Buckley, F., Holland, J.G., 1974. Petrology and geochemistry of Easter Island. Contrib. Mineral. Petrol. 44 (2), 85–100.

Barnicoat, A.C., Fry, N., 1986. High-pressure metamorphism of the Zermatt-Saas ophiolite zone, Switzerland. J. Geol. Soc. 143, 607–618.

Batiza, R., Niu, Y., 1992. Petrology and magma chamber processes at the East Pacific Rise 9°30′N. J. Geophys. Res. 97, 6779–6797.

Bonnand, P., Parkinson, I.J., Annand, M., 2016. Mass dependent fractionation of stable chromium isotopes in mare basalts: implications for the formation and the differentiation of the Moon. Geochim. Cosmochim. Acta 175, 208–221.

Brenan, J.M., Shaw, H.F., Phinney, D.L., Ryerson, F.J., 1994. Rutile-fluid partitioning of Nb, Ta, Zr, U and Th: implications for high-field-strength element depletions in island-arc basalts. Earth Planet. Sci. Lett. 128, 327–339.

Canup, R.M., 2012. Forming a Moon with an Earth-like composition via a giant impact. Science 338, 1052–1055.

Clayton, R.N., 1993. Oxygen isotopes in meteorites. Annu. Rev. Earth Planet. Sci. 21, 115–149.

Clayton, R.N., Hurd, J.M., Mayeda, T.K., 1973. Oxygen isotopic compositions of Apollo 15, 16, and 17 samples, and their bearing on lunar origin and petrogenesis. In: Proc. 4th Lunar Sci. Conf., pp. 1535–1542.

Cúk, M., Stewart, S.T., 2012. Making the Moon from a fast-spinning Earth: a giant impact followed by resonant despinning. Science 338, 1047–1052.

Dale, C.W., Gannoun, A., Burton, K.W., Argles, T.W., Parkinson, I.J., 2007. Rhenium–osmium isotope and elemental behaviour during subduction of oceanic crust and the implications for mantle recycling. Earth Planet. Sci. Lett. 177, 211–225.

Dauphas, N., Marty, B., Resiberg, L., 2002. Molybdenum nucleosynthetic dichotomy revealed in primitive meteorites. Astrophys. J. 569, L139–L142.

Dauphas, N., Burkhardt, C., Warren, P.H., Teng, F.-Z., 2014a. Geochemical arguments for an Earth-like Moon-forming impactor. Philos. Trans. R. Soc. A 372, 20130244. http://dx.doi.org/10.1098/rsta.2013.0244.

Dauphas, N., Roskosz, M., Alp, E.E., Neuville, D.R., Hu, M.Y., Sio, C.K., Tissot, F.L.H., Zhao, J., Tissandier, L., Médard, E., Cordier, C., 2014b. Magma redox and structural controls on iron isotope variations in Earth's mantle and crust. Earth Planet. Sci. Lett. 398, 127–140.

Debret, B., Andreani, M., Muñoz, M., Bolfan-Casanova, N., Carlut, J., Nicollet, C., Schwartz, S., Trcera, N., 2014. Evolution of Fe redox state in serpentine during subduction. Earth Planet. Sci. Lett. 400, 206–218.

Dempsey, S.R., 2012. Geochemistry of the volcanic rocks form the Sunda arc. PhD thesis. Durham University.

Elkins-Tanton, L.T., Van Orman, J.A., Hager, B.H., Grove, T.L., 2002. Re-examination of the lunar magma ocean cumulate overturn hypothesis: melting or mixing is required. Earth Planet. Sci. Lett. 196, 239–249.

Elkins-Tanton, L.T., Hagger, B.H., Grove, T.L., 2004. Magmatic effects of the lunar late heavy bombardment. Earth Planet. Sci. Lett. 222, 17–27.

Escrig, S., Capmas, F., Dupré, B., Allégre, C.J., 2004. Osmium isotopic constraints on the nature of the DUPAL anomaly from Indian mid-ocean-ridge basalts. Nature 431, 59–63.

Farges, F., Brown Jr., G.E., Rehr, J.J., 1996. Coordination chemistry of Ti (IV) in silicate glasses and melts: I. XAFS study of titanium coordination in oxide model compounds. Geochim. Cosmochim. Acta 60 (16), 3023–3038.

Farges, F., Brown Jr., G.E., 1997. Coordination chemistry of titanium (IV) in silicate glasses and melts: IV. XANES studies of synthetic and natural volcanic glasses and tektites at ambients temperature and pressure. Geochim. Cosmochim. Acta 61 (9), 1863–1870.

Gao, J., John, T., Klemd, R., Xiong, X.M., 2007. Mobilization of Ti–Nb–Ta during subduction: evidence from rutile-bearing dehydration segregations and veins hosted in eclogite, Tianshan, NW China. Geochim. Cosmochim. Acta 71, 4974–4996.

Greber, N.D., Dauphas, N., Millet, M.-A., Putchel, I.S., 2016. The titanium isotope composition of chondrites and Earth. In: Lunar and Planetary Science XL. Abstract #1448.

Gualda, G.A.R., Ghiorso, M.S., Lemons, R.V., Carley, T.L., 2012. Rhyolite-MELTS: a modified calibration of MELTS optimized for silica-rich, fluid-bearing magmatic systems. J. Petrol. 53, 875–890.

Hallis, L.J., Annand, M., Strekopytov, S., 2014. Trace-element modeling of mare basalt parental melts: implications for a heterogeneous lunar mantle. Geochim. Cosmochim. Acta 134, 289–316.

Heimann, A., Beard, B.L., Johnson, C.M., 2008. The role of volatile exsolution and subsolidus fluid/rock interactions in producing high $^{56}Fe/^{54}Fe$ ratios in siliceous igneous rocks. Geochim. Cosmochim. Acta 72, 4379–4396.

Hess, P.C., Parmentier, E.M., 1995. A model for the thermal and chemical evolution of the Moon's interior: implications for the onset of mare volcanism. Earth Planet. Sci. Lett. 134, 501–514.

Kessel, R., Schmidt, M.W., Ulmer, P., Pettke, T., 2005. Trace element signature of subduction-zone fluids, melts and supercritical liquids at 120–180 km depth. Nature 437, 724–727.

Krawczynski, M.J., Sutton, S.R., Grove, T.L., Newville, M., 2009. Titanium oxidation state and coordination in the lunar high-titanium glass source mantle. In: Lunar and Planetary Science XL. Abstract #2164.

Krawczynski, M.J., Millet, M.-A., Dauphas, N., Van Orman, J.A., 2013. The mare basalt Fe-isotope dichotomy: a preliminary exploration into the role of ilmenite fractionation. In: Lunar and Planetary Science XLIV. Abstract #2620.

Liu, Y., Spicuzza, M.J., Craddock, P.R., Day, J., Valley, J.W., Dauphas, N., Taylor, L.A., 2010. Oxygen and iron isotope constraints on near-surface fractionation effects

and the composition of lunar mare basalt source regions. Geochim. Cosmochim. Acta 74, 6249–6262.
Ludwig, K., 2003. ISOPLOT: a geochronological toolkit for Microsoft Excel 3.00. Berkeley Geochronology Center Special Publication No. 4, Berkeley, CA 94709.
Lugmair, G., Shukolyukov, A., 1998. Early Solar System timescales according to ^{53}Mn–^{53}Cr systematics. Geochim. Cosmochim. Acta 62, 2863–2886.
Lundstrom, C.L., 2009. Hypothesis for the origin of convergent margin granitoids and Earth's continental crust by thermal migration zone refining. Geochim. Cosmochim. Acta 73, 5709–5729.
Mastrobuono-Battisti, A., Perets, H.B., Raymond, S., 2015. A primordial origin for the compositional similarity between the Earth and the Moon. Nature 520, 212–215.
McDonough, W.F., 1991. Partial melting of subducted oceanic crust and its residual eclogitic lithology. Philos. Trans. R. Soc. Lond. Ser. A, Math. Phys. Sci. 335, 407–418.
McDonough, W.F., Sun, S.-S., 1995. The composition of the Earth. Chem. Geol. 120, 223–253.
Millet, M.-A., Dauphas, N., 2014. Ultra-precise titanium stable isotope measurements by double-spike high resolution MC-ICP-MS. J. Anal. At. Spectrom. 2014 (29), 1444–1458.
Millet, M.-A., Doucelance, R., Schiano, P., David, K., Bosq, C., 2008. Mantle plume heterogeneity versus shallow-level interactions: a case study, the São Nicolau Island, Cape Verde archipelago. J. Volcanol. Geotherm. Res. 176 (2), 265–276.
Millet, M.-A., Doucelance, R., Baker, J.A., Schiano, P., 2009. Reconsidering the origins of isotopic variations in Ocean Island Basalts: insights from fine-scale study of São Jorge Island, Azores archipelago. Chem. Geol. 265 (3–4), 289–302.
Niederer, F.R., Papanastassiou, D.A., Wasserburg, G.J., 1980. Endemic isotopic anomalies in titanium. Astrophys. J. 240, L73–L77.
Nielsen, R.L., Beard, J.S., 2000. Magnetite–melt HFSE partitioning. Chem. Geol. 164, 21–34.
Niemeyer, S., 1988. Isotopic diversity in nebular dust: the distribution of Ti isotopic anomalies in carbonaceous chondrites. Geochim. Cosmochim. Acta 52, 2941–2954.
Pahlevan, K., Stevenson, D.J., 2007. Equilibration in the aftermath of the lunar-forming giant impact. Earth Planet. Sci. Lett. 262, 438–449.
Paniello, R.C., Day, J.M., Moynier, F., 2012. Zinc isotopic evidence for the origin of the Moon. Nature 490, 376–379.
Pearson, D.G., Irvine, G.J., Ionov, D.A., Boyd, F.R., Dreibus, G.E., 2004. Re–Os isotope systematics and platinum group element fractionation during mantle melt extraction: a study of massif and xenolith peridotite suites. Chem. Geol. 208, 29–59.
Poitrasson, F., Freydier, R., 2005. Heavy iron isotope composition of granites determined by high resolution MC-ICP-MS. Chem. Geol. 222, 132–147.
Poitrasson, F., Halliday, A.N., Lee, D-C., Levasseur, S., Teutsch, N., 2004. Iron isotope differences between Earth, Moon, Mars and Vesta as possible records of contrasted accretion mechanisms. Earth Planet. Sci. Lett. 223, 253–266.
Prytulak, J., Elliott, T., 2007. TiO_2 enrichment in ocean island basalts. Earth Planet. Sci. Lett. 263, 388–403.
Puchelt, H., Emmermann, R., 1983. Petrogenetic implications of tholeiitic basalt glasses from the East Pacific Rise and the Galápagos Spreading Center. Chem. Geol. 38, 39–56.
Rapp, J.F., Klemme, S., Butler, I.B., Harley, S.L., 2010. Extremely high solubility of rutile in chloride and fluoride-bearing metamorphic fluids: an experimental investigation. Geology 38, 323–326.
Reinecke, T., 1991. Very-high-pressure metamorphism and uplift of coesite bearing metasediments from the Zermatt-Saas zone, Western Alps. Eur. J. Mineral. 3 (1), 7–17.
Reufer, A., Meier, M.M., Benz, W., Wieler, R., 2012. A hit-and-run giant impact scenario. Icarus 221, 296–299.
Ringwood, A.E., Kesson, S.E., 1976. A dynamic model for mare basalt petrogenesis. In: Proc. Lunar Planet. Sci. Conf. 7th, pp. 1697–1722.
Schauble, E.A., 2004. Applying stable isotope fractionation theory to new systems. In: Johnsos, C.M., Beard, B.L., Albarede, F. (Eds.), Geochemistry of Non-traditional Stable Isotopes, vol. 55, pp. 65–111.
Sedaghatpour, F., Teng, F-Z., Liu, Y., Sears, D.W., Taylor, L.A., 2013. Magnesium isotopic composition of the Moon. Geochim. Cosmochim. Acta 120, 1–16.
Seitz, H-M., Brey, G.P., Weyer, S., Durali, S., Ott, U., Münker, C., Mezger, K., 2006. Lithium isotope compositions of Martian and lunar reservoirs. Earth Planet. Sci. Lett. 245, 6–18.
Sharp, Z., Shearer, C., McKeegan, K., Barnes, J., Wang, Y., 2010. The chlorine isotope composition of the Moon and implications for an anhydrous mantle. Science 329, 1050–1053.
Simon, S.B., Sutton, S.R., Grossman, L., 2014. Valence of Ti in lunar igneous rocks: The first direct measurements. In: Lunar and Planetary Science XLV. Abstr. #1063.
Snyder, G.A., Taylor, L.A., Neal, C.R., 1992. A chemical model for generating the sources of mare basalts: combined equilibrium and fractional crystallization of the lunar magmasphere. Geochim. Cosmochim. Acta 56, 3809–3823.
Sossi, P.A., Foden, J.D., Halverson, G.P., 2012. Redox-controlled iron isotope fractionation during magmatic differentiation: an example from the Red Hill intrusion, S. Tasmania. Contrib. Mineral. Petrol. 164, 757–772.
Telus, M., Dauphas, N., Moynier, F., Tissot, F.L.H., Teng, F-Z., Nabelek, P.I., Craddock, P.R., Groat, L.A., 2012. Iron, zinc, magnesium and uranium isotopic fractionation during continental crust differentiation: the tale from migmatites, granitoids, and pegmatites. Geochim. Cosmochim. Acta 97, 247–265.
Trinquier, A., Elliott, T., Ulfbeck, D., Coath, C., Krot, A.N., Bizzarro, M., 2009. Origin of nucleosynthetic isotope heterogeneity in the solar protoplanetary disk. Science 324, 374–376.
Turner, S., Hawkesworth, C., Rogers, N., King, P., 1997. U–Th isotope disequilibria and ocean island basalt generation in the Azores. Chem. Geol. 139 (1–4), 145–164.
Van Orman, J.A., Grove, T.L., 2000. Origin of lunar high-titanium ultramafic glasses: constraints from phase relations and dissolution kinetics of clinopyroxene-ilmenite cumulates. Meteorit. Planet. Sci. 35, 783–794.
Wade, J., Wood, B.J., 2001. The Earth's 'missing' niobium may be in the core. Nature 409, 75–78.
Wadhwa, M., 2008. Redox conditions on small bodies, the Moon and Mars. Rev. Mineral. Geochem. 68, 493–510.
Wagner, T.P., Grove, T.L., 1997. Experimental constraints on the origin of lunar high-Ti ultramafic glasses. Geochim. Cosmochim. Acta 61, 1315–1327.
Weyer, S., Anbar, A.D., Brey, G.P., Munker, C., Mezger, K., Woodland, A.B., 2005. Iron isotope fractionation during planetary differentiation. Earth Planet. Sci. Lett. 240, 251–264.
Williams, N.H., Schönbächler, M., Fehr, M.A., Akram, W.M., Parkinson, I.J., 2014. Different heterogeneously distributed titanium isotope components in solar system materials and mass-dependent titanium isotope variations. In: Lunar and Planetary Science XL. Abstract #2183.
Yi, W., Halliday, A.N., Alt, J.C., Lee, D.C., Rekhamper, M., Garcia, M.O., Su, Y.J., 2000. Cadmium, indium, tin, tellurium, and sulfur in oceanic basalts: implications for chalcophile element fractionation in the Earth. J. Geophys. Res. 105, 18927–18948.
Zhang, J., Dauphas, N., Davis, A.M., Pourmand, A., 2011. A new method for MC-ICPMS measurement of titanium isotopic composition: identification of correlated isotope anomalies in meteorites. J. Anal. At. Spectrom. 26, 2197–2205.
Zhang, J., Dauphas, N., Davis, A.M., Leya, I., Fedkin, A., 2012. The proto-Earth as a significant source of lunar material. Nat. Geosci. 5, 251–255.
Zhang, J., Huang, S., Davis, A.M., Dauphas, N., Hashimoto, A., Jacobsen, S.B., 2014. Calcium and titanium isotopic fractionations during evaporation. Geochim. Cosmochim. Acta 140, 365–380.